Army Research Laboratory

Aberdeen Proving Ground, MD 21005-5069

Viscoelastic and Transport Properties of Sulfonated PS-PIB-PS Block Copolymers

Eugene Napadensky, Dawn Crawford, James Sloan, and Nora Beck Tan
Weapons and Materials Research Directorate, ARL

Abstract

Morphology, viscoelastic, and transport properties of the sulfonated polystyrene-polyisobutylene-polystyrene (PS-PIB-PS) block copolymer were investigated with respect to sulfonation level and counter-ion substitution. Dynamic mechanical analysis (DMA) was used to examine the dynamic storage modulus E' and dynamic loss modulus E'', as they relate to changes in sulfonation levels. Small-angle x-ray scattering (SAXS) results confirmed that at a certain percent of sulfonation, a phase transition occurs from hexagonally packed cylinders to lamellar structure due to swelling of the styrene domains caused by the higher sulfonation levels. Transport measurements using Fourier Transfer Infrared Spectrometer (FTIR) confirm that the sulfonation level directly dictates the transport rate of small molecules (alcohol and water) through the PS-PIB-PS triblock copolymer membrane. Faster water transport can be achieved by incorporating more sulfonic acid groups throughout the polymer backbone. In addition, infrared (IR) data clearly identifies molecular interactions between the solvating alcohol molecules and the PS-PIB-PS triblock copolymer. The observed properties suggest that these ion-containing block copolymers are worthy of further development as barrier membranes to be incorporated into chemical protective clothing.

Contents

INTENTIONALLY LEFT BLANK.

List of Figures

List of Tables

1. Introduction

The U.S. Army requires that all fielded systems be survivable in a chemical warfare environment. Butyl rubber is currently used in standard protective clothing because it provides good protection from chemical and biological agents. However, the bulky and impermeable nature of butyl rubber results in unacceptable levels of stress on the soldier [1]. Outfitting the soldier in accordance with new Future Combat System (FCS) and Objective Force guidelines requires that the materials be lightweight and flexible, enabling the soldier to move freely. In an effort to address these requirements, a series of sulfonated triblock copolymers have been developed. The novel block copolymers exhibit flexibility over a broad temperature range and selectively permeable "membrane-like" characteristics.

2. Background

A novel class of self-assembled block copolymers has been developed and investigated. These materials exhibit transport and mechanical properties necessary for potential consideration as advanced materials for soldier clothing. The novel polymers are comprised of triblocks of polystyrene-polyisobutylene-polystyrene (PS-PIB-PS). The major component of the copolymer is polyisobutylene (PIB), lending low temperature flexibility to the material and good barrier properties. Polystyrene (PS) forms the glassy component, which physically crosslinks the PIB providing mechanical integrity. In the solid state, the thermodynamic immiscibility of the two components results in spontaneous microphase separation where domains of PS are formed in the rubbery PIB matrix. The fraction of PS controls the morphology that is formed in the copolymer which can be cylinders, lamellae, or spheres [2]. The PS-PIB-PS triblock copolymer under investigation is comprised of approximately 30% PS and the resulting morphology is cylinders in the unsulfonated form. The cylindrical morphology formed by the PS fraction provides a channel by which molecular transport across a film can occur while the PIB matrix acts as a chemical barrier. Ionomeric modification of the commercially available PS-PIB-PS block copolymers (TS-3000S) was performed by sulfonation of the styrene monomers to varying levels [3]. The modified copolymer exhibits hydrophilic character, and its ability to transport water has been demonstrated. Likewise, preliminary experiments have been performed which show that the films are selective in blocking organic compounds. Ionomeric modification of the polymer

1

causes association of ion rich domains [4, 5] and results in a stiffer material without significantly affecting the glass transition temperature. Thus, the material remains flexible and transparent following chemical modification.

The PS-PIB-PS block copolymer in the unmodified and ionomeric forms readily dissolves in selected organic solvents, making large-scale processing economically feasible. Over the past year, we have focused on the control of polymer morphology as a result of processing and level of sulfonation of the styrene monomers. Our earlier processing studies showed that slower solvent evaporation times leads to improved long range order. However, these changes in morphology do not affect the permeation properties of the copolymer. Our studies show that in the unmodified form, the block copolymer behaves as a barrier material, blocking water and polar organic compounds. Ionomeric modification via sulfonation of styrenic components of the polymer chain disrupts the morphology; however, self-assembly occurs in the PS-PIB-PS triblock copolymer irregardless of the processing method or the level of sulfonation. We have demonstrated that solution processing of sulfonated PS-PIB-PS under nonequilibrium conditions (solvent casting or spraying) results in films with a microphase separated morphology and permselective characteristics. Our earlier work on the control of solvent evaporation is discussed elsewhere [6]. The final report presented here, details our subsequent investigations on the effect of sulfonation level and counter-ion substitution on the morphology, transport, and mechanical properties of the block copolymer.

3. Discussion

3.1 Morphology

3.1.1 Small Angle X-ray Scattering

Materials examined were solution cast films of unmodified PS-PIB-PS triblock copolymer and sulfonated PS-PIB-PS triblocks with styrene sulfonic acid levels in the styrenic phase ranging from 5% to 26%. One sample that had been subjected to ion exchange treatment in an aqueous solution of zinc salt was also examined. These films were cast according to procedures outlined previously. Small angle x-ray scattering (SAXS) patterns were collected at the National Synchrotron Light Source at Brookhaven National Laboratory, Brookhaven, NY, using pinhole collimation and a two-dimensional (2-D) multiwire type area detector. SAXS images were circularly averaged using commercial software routines.

For copolymers comprised of strongly immiscible blocks, such as the PS-PIB-PS triblocks, microphase segregation will occur via self-assembly, resulting in the

2

formation of ordered structures having characteristic dimensions on the nanoscale. The type of ordered structure that forms is dictated by the relative volume fractions of the two components in the system. For example, for ideal systems with minor component composition in the 25–40 volume-percent range, microphase segregated morphologies with cylinders of the minor component hexagonally arranged within a "matrix" of the major component are formed (see Figure 1) [7]. Volume fractions of minor components in the 19–25% range typically yield body-centered cubic microphases, while systems in which the volume fractions of both components are similar form lamellar structures. Morphology is generally elucidated experimentally using small angle scattering experiments which show distinct, characteristic patterns for different microstructures. Transmission electron microscopy is often used to corroborate findings, particularly if the small angle scattering patterns show weak or poorly defined features, or if the system forms complex phases.

THEORIES FOR MELT PHASE BEHAVIOUR
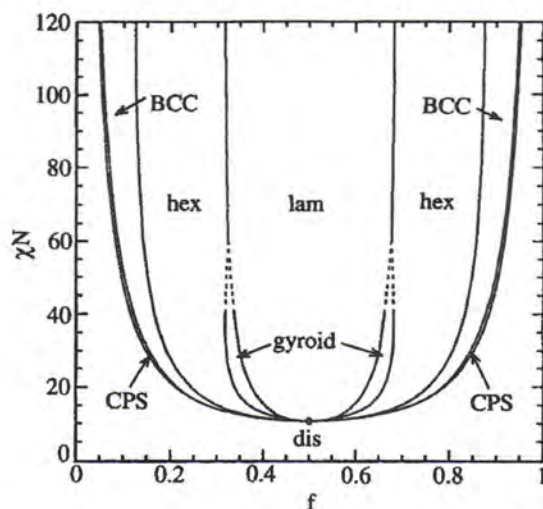
MELT PHASE BEHAVIOUR OF BLOCK COPOLYMERS
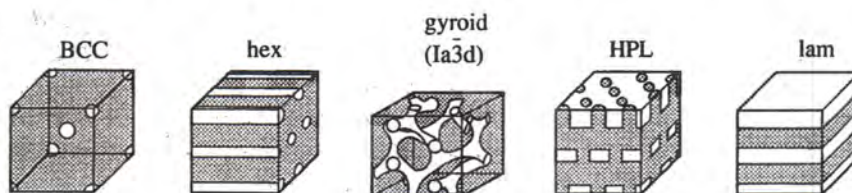
Figure 1. Morphology diagram for microphase segregation in block copolymers.

3

For this study, the microphase morphology is important because it controls the connectivity and arrangement of the proposed transport pathways—the sulfonated styrene domains—and may also significantly influence the mechanical performance in the system. Characterization of the morphology is also particularly important for this study since previous work has suggested that competition between sulfonic acid group aggregation within the styrenic microphase can compete with self-assembly in the block copolymer. This competition may result in disruption in the development of the ordered structure in the materials [6], or the formation of morphologies different from those predicted based simply on component volume fractions [2, 8].

The unmodified triblock copolymer starting materials studied in this program contain 29 volume-percent of the minor component, styrene, and thus should form hexagonally packed cylindrical phases. The SAXS patterns from hexagonally packed cylindrical phases are characterized by a strong low angle peak occurring at a scattering vector position designated as q^*, and higher order peaks occurring at scattering vector positions $\sqrt{3}q^*$, $\sqrt{4}q^*$, $\sqrt{7}q^*$, and $\sqrt{9}q^*$. The PS-PIB-PS copolymers used in this study exhibit this characteristic pattern, unambiguously identifying the microphase segregated structure as hexagonally packed cylinders (Figure 2). The position of the first peak is at $q^* = 0.0248$ Å^{-1}, indicating that the (100) spacing in the structure is 253.4 Å, corresponding to a hexagonal lattice constant of $a = 219.5$ Å.
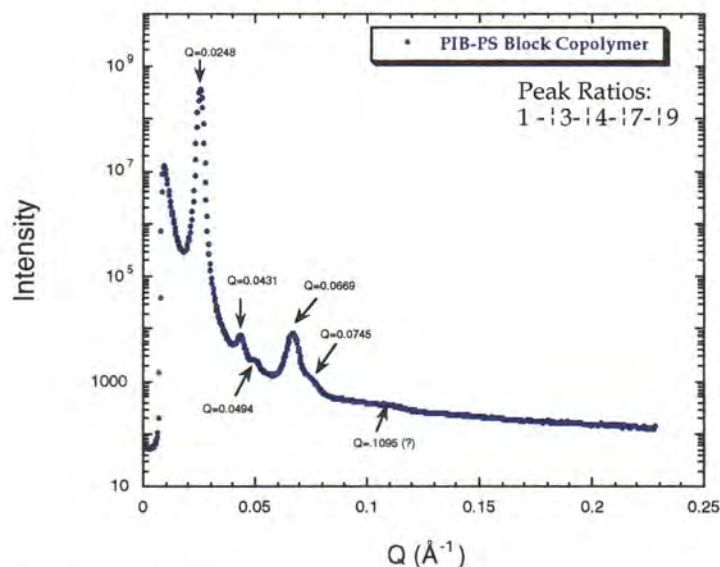
Figure 2. Small angle x-ray scattering pattern from the unmodified PS-PIB-PS copolymer film.

All sulfonated copolymers examined as part of this investigation displayed SAXS patterns characteristic of microphase segregated structures, indicating that sulfonation did not disrupt the self-assembly process to the extent that self-assembly was suppressed. In addition, the SAXS patterns of these copolymer films displayed more order than some previously prepared in our laboratory [6], which we believe to be due to improvements in film processing methods. The first order peak positions for the copolymers increase slightly with sulfonation, with the maximum occurring for the most highly sulfonated material studied. The peak position for this 26% sulfonated copolymer was $q_{26}^* = 0.0201$ Å^{-1}, corresponding to $d_{100} = 313$ Å, which represents an increase of (coincidentally) ~26% in d_{100} relative to the unmodified PS-PIB-PS triblock.

Two different types of patterns were observed from the sulfonated copolymers. The first pattern, which is similar to that observed for the unmodified copolymers, is displayed by copolymers having either 5% or 8% of their styrene monomers converted to styrene sulfonic acid (5% or 8% sulfonation level) and having been cast from pure toluene solvent (Figure 3). This is the characteristic pattern of a hexagonally packed cylindrical structure. The increased breadth of the first order peak q* and low scattering intensity of the higher order peaks indicates that the long range order in the sulfonated copolymers is poor in comparison with that displayed by the unsulfonated starting material.

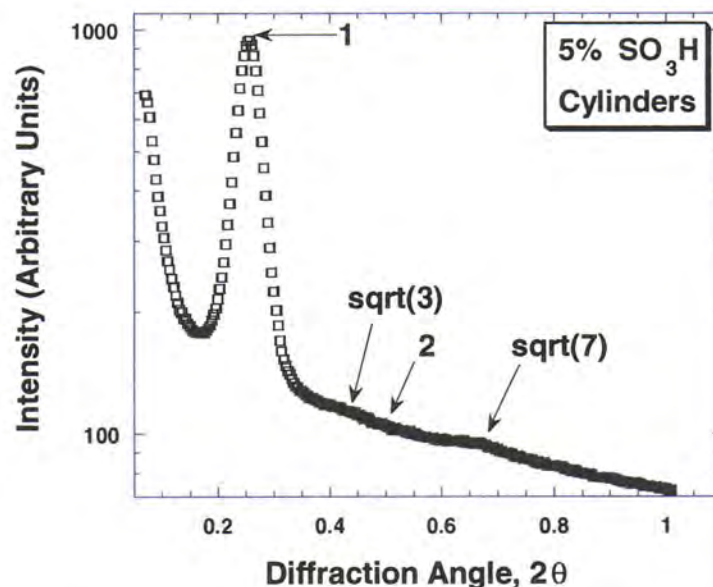
Figure 3. Small angle x-ray scattering patterns from 5% sulfonated PS-PIB-PS triblock copolymer.

For copolymers with sulfonation levels of 12–26% cast from hexanol/toluene mixtures, a different characteristic SAXS pattern is recorded. These patterns display 2–6 characteristic peaks, with the first occurring at a position designated q^* and the second through sixth occurring at positions which are integral multiples of q^* (Figure 4). These patterns are indicative of a lamellar structure which characteristically display peaks at positions q^*, $2q^*$, $3q^*$, $4q^*$, etc. It is not uncommon for some higher order peaks to be weak or absent, as with $3q^*$ in Figure 4, due to coincidence with minima in scattering features associated with isolated substructural features within the material. The first order peaks in the 14–26% sulfonated copolymers are broad relative to the unmodified copolymer's first order peak, as are first order peaks in the 5% and 8% sulfonated copolymers.
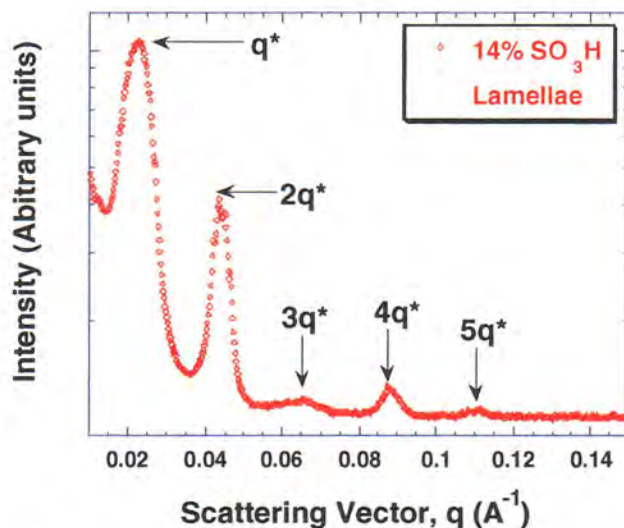
Figure 4. Small angle x-ray scattering pattern from 14% sulfonated PS-PIB-PS triblock copolymer.

Lamellae are typically seen in systems in which the volume fractions of the two components are more nearly equal than the 29/71 ratio of our starting materials. Given that the sulfonation process itself is not expected to significantly increase the volume of the styrenic phase, the observed transition from the hexagonally packed cylindrical phase to the lamallar microphase was somewhat unexpected. However, transitions to structures with higher *apparent* styrene volume fractions have been previously documented for other sulfonated styrene-olefin copolymer systems [5]. There are two primary factors that contribute to the morphology transition. First, we chose to cast the copolymers that were sulfonated to levels of 12% or more from toluene/hexanol mixtures rather than pure toluene. This was necessary due to changes in solubility of the copolymers as the sulfonation level, and correspondingly the polarity, increased in the styrenic phase. However, the hexanol selectively solvates the sulfonated styrene block, which

effectively swells that block during the casting process, thereby altering morphology. Previously documented are instances in which the selectivity of a solvent toward a specific segment in a block copolymer has resulted in a morphology transition [9–11]. The morphology transition that would be expected in the current system as a result of selective solvation of the sulfonated styrene microphase by hexanol would be from cylinders to lamallae, as observed. In addition to selective solvent effects, the tendency for aggregation of the acidic groups may also favor the cylinder to lamallae transition by hindering organization and packing of the copolymers during the self-assembly process [2, 8]. Though the change in casting solvent may be primarily responsible for the formation of the nonequilibrium lamallar phase in the highly sulfonated systems, it is possible that the aggregation of the acid groups act to stabilize this structure once it is formed and prevent reversion back to the thermodynamically favored cylindrical phase upon annealing or postcasting treatment. Reversion of nonequilibrium morphologies induced by selective solvent effects to more stable structures during annealing has been documented in other systems [9].

As part of our most recent efforts, the morphology of ion-exchanged sulfonated PS-PIB-PS block copolymers was studied by small angle scattering. The intensity vs. scattering vector for a copolymer with 22.5% sulfonation which was treated to foster exchange of the acidic proton with zinc is given in Figure 5; it illustrates the lamellar structural features of this self-assembled system. The ion-exchange process did not disrupt the self-assembly or alter the morphology in this system, though these effects have been observed in other block copolymer ionomer systems [5]. The first order peak occurs at $q_{22.5Zn}^* = 0.0200$ Å^{-1}, corresponding to $d_{100} = 315$ Å, which is a slight increase over the spacing for the same sulfonated copolymer in the acidic form $d_{100} = 294$ Å.
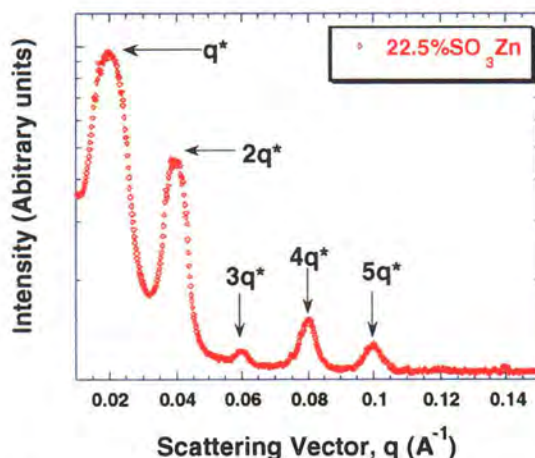

Figure 5. Small angle x-ray scattering pattern from 22.5% sulfonated PS-PIB-PS triblock copolymer ion exchanged with zinc.

The second region of interest in the scattering from the Zn ionomer is in the higher q range of 0.1–0.2 Å^{-1} (not shown), which is where the peak due to interparticle interference between ionic clusters would appear. A weak scattering peak occurs at $q_{cluster}$ = 0.183 Å^{-1}, corresponding to a cluster spacing of $d_{cluster}$ = 34.3 Å. This feature size is consistent with cluster sizes observed previously in sulfonated polystyrene ionomers and sulfonated block copolymer ionomers [5, 8] and arises from interparticle interference between zinc clusters residing within the sulfonated polystyrene microphase. The appearance of this feature is direct evidence that the exchange process used to substitute zinc ions for acidic protons within the copolymers was successful.

3.1.2 Dynamical Mechanical Analysis (DMA)

The DMA experiments were performed on films cast from 5% polymer solutions of toluene or toluene/hexyl alcohol mixtures of PS-PIB-PS triblock copolymers with varying degrees of styrene sulfonic acid. Specifically, the levels of sulfonation in the cast films were 0% (unmodified triblock copolymer), 5%, 8%, 12%, 14%, 17%, and 22%. Figure 6 shows the storage modulus (E') vs. temperature for this series of polymers. These data show that the differences in E' for the unmodified triblock copolymer and that of the copolymers sulfonated at 5% and 8% is negligible, suggesting that sulfonation levels up to 8% do not affect the dynamic modulus of the block copolymers. However, block copolymers sulfonated to higher levels (12%, 14%, 17%, and 22%) exhibit a significant increase in the rubbery plateau modulus, indicating increased stiffness of the polymers. These data are consistent with a change in morphology from hexagonally packed cyclinders (0%, 5%, and 8% sulfonation) to lamellar structure (12%, 14%, 17%, and 22% sulfonation), which was confirmed by small angle x-ray scattering (SAXS) as discussed earlier. Lamellar structure of the rigid styrenic components existing parallel to the film plane would conceivably increase stiffness of the polymer above the glass transition temperature (Tg). The higher percentages of styrene sulfonic acid effectively increase the volume fraction of the styrenic portions of the polymer above 30% and into the lamellar region of the phase diagram (Figure 1), resulting in higher E'. The significant increase in E' for the block copolymers sufonated above 8% can be further explained by the increased interaction of the sulfonic acid groups that act as thermally reversible, noncovalent crosslinks in the hard domains [4, 5].

Figure 7 shows the dynamic loss modulus (E") for the series of block copolymers. E" provides information on the low temperature flexibility and Tg of the triblock copolymers. These data indicate that although the sulfonation level significantly affects the modulus of the polymers due to the contributions from the rigid PS components of the polymer chain, the low temperature properties of the block copolymer are virtually unaffected. The primary peak associated with the glass
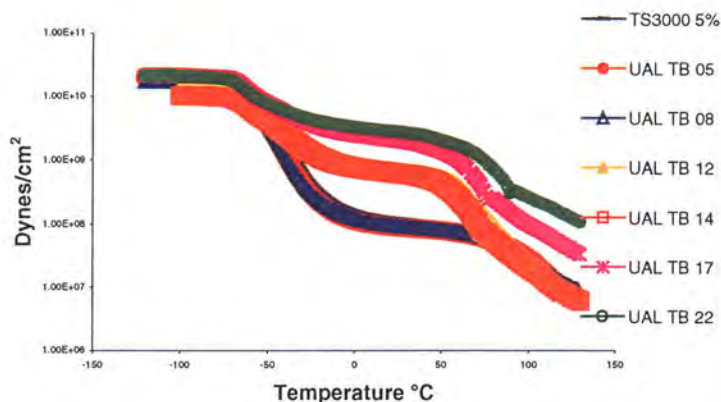
Figure 6. Effect of sulfonation level on E′.
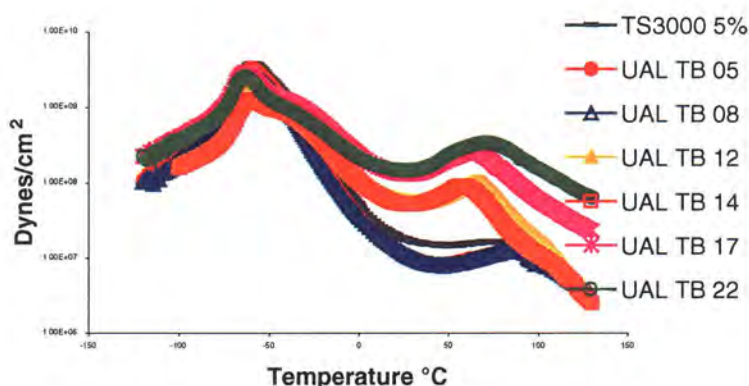
Figure 7. Effect of sulfonation on E″.

transition retains its peak magnitude at approximately –60 °C, irregardless of the sulfonation level. Thus, the flexible, elastomeric behavior of the polymer is not compromised as a result of increasing sulfonation level.

The loss characteristics of the sulfonated copolymers are also shown in the tan δ vs. temperature plot (Figure 8). The predominant peak shown in the low temperature region shows the glass transition for the PIB domain. It can be seen that the amorphous "elastomeric" nature of the block copolymer is unaffected by the sulfonation level of 5% and 8% as the peak magnitude for these systems is relatively unchanged compared to the unmodified polymer. As the sulfonation level is increased beyond 8%, a significant drop in the peak magnitude occurs, and two distinct features of the peak can be seen. One feature is a low temperature shoulder that is most likely due to "unrestricted" PIB chains, and a

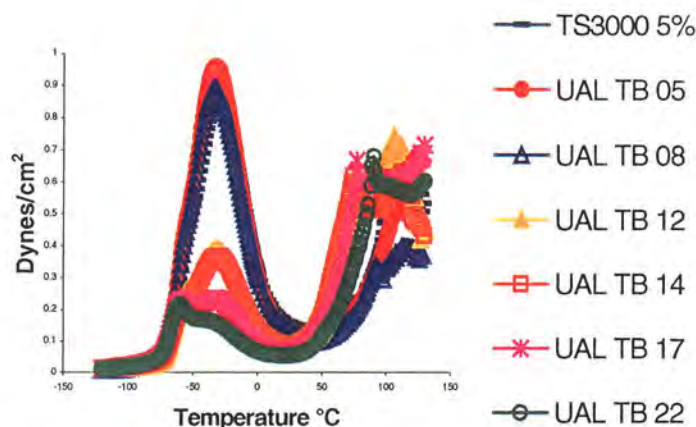Figure 8. Effect of sulfonation on tan δ.

higher temperature peak that is believed to be the result of PIB chains near the PIB-PS interface. This observation has also been made by other researchers investigating similar block copolymers [12]. As the sulfonation level in these systems increases, a greater degree of physical crosslinking occurs via hydrogen bonding between adjacent sulfonic acid groups. The hydrogen bond "crosslinks" in the PS domain restrain molecular motion of the PIB chains near the PIB/PS interface, and thus the viscous loss associated with the relaxation of these chains is reduced. The theory of restricted polymer chain mobility in the vicinity of an ionic multiplet has been reported in the literature [12, 13]. However, the hydrogen bond association occurs in the minor portion of the block copolymer, and thus the overall Tg of the PIB domain is relatively unaffected. Also, the low temperature shoulder of this transition is related to the "pure" PIB domains and is unaffected by the association within the PS domains.

Investigations were also performed on the triblock copolymer sulfonated to 22% with the acidic hydrogen substituted with Zn and tetrabutylammonium organic counter ions. The E' of these systems is shown in Figure 9. Both counter-ion substituted systems exhibit improved temperature stability, as can be seen in the rubbery plateau region of the curves. This effect is less prominent in the organic counter-ion substituted polymer, which shows only a slight increase in Tg of the PS domain compared to the acid form of the polymer. However, the Zn substituted polymer exhibits excellent heat stability, with no sign of softening up to the end point of the experiment at 130 °C. This is consistent with data on other Zn substituted ionomers previously reported in the literature and is the result of the stronger ionic bonds formed in this system compared to the hydrogen bonding present in the acid form of the polymer [4, 5, 14].
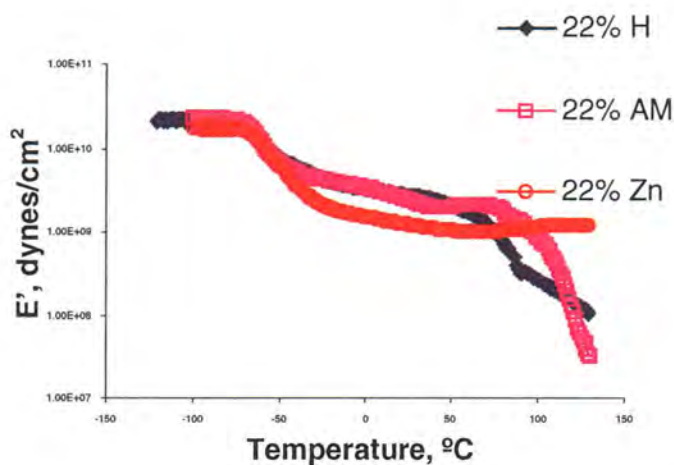
Figure 9. Effect of counter-ion on E' for samples sulfonated to 22%.

The loss modulus of these copolymers is shown in Figure 10. Here it can be seen that the counter-ion substitution does not adversely affect the low temperature PIB transition, which is present at approximately –60 °C. In the high temperature region of the curve, the increase in Tg for the organic counter-ion substituted polymer is apparent compared to the acid form of the copolymer. The relatively flat curve for the Zn substituted copolymer in the same region indicates that that system does not undergo a Tg below 130 °C.
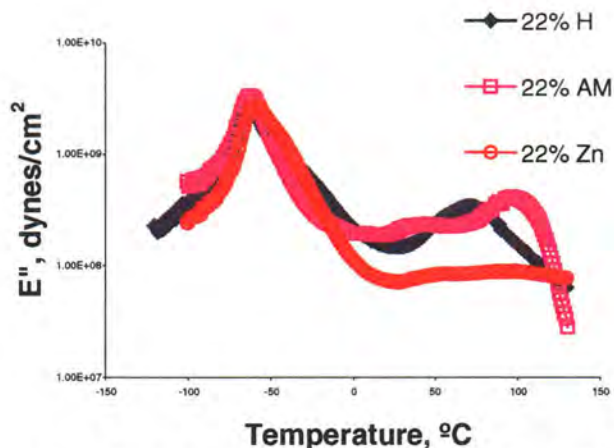

Figure 10. Effect of counter-ion on E" for samples sulfonated to 22%.

Tan δ for the counter-ion substituted systems is shown in Figure 11. In the acid form, the low temperature transition exhibits the two distinct features as discussed earlier. Counter-ion substitution with the organic cation results in a narrower glass transition with no higher temperature feature, thus indicating
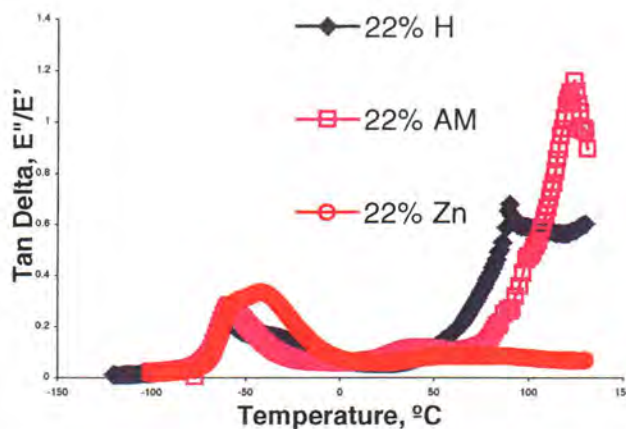
11

Figure 11. Effect of counter-ion on tan δ for samples sulfonated to 22%.

that this system has less restriction of the PIB chains at the PS domain interface. This may be due to inhibition of ion association in the PS domain because the bulky ammonium ion may create steric hinderance. This occurrance would also explain the dramatic drop in E' of that system following the T_g of the PS domains as shown in Figure 9, and the reduced breadth of the rubbery plateau compared to the Zn counter-ion substituted copolymers. These observations are consistent with other findings [15]. The PIB glass transition of the Zn counter-ion substituted copolymer is distinctly broader than the organic cation or acid forms of the copolymer. However, the Zn substituted system does exhibit the two-featured transition. The tan δ magnitude of the transition associated with restricted PIB chains is larger for the Zn substituted copolymer compared to the acid form of the polymer. This may be the result of more strongly associated PS domains in the Zn substituted system, resulting in improved phase separation in the block copolymer and thus greater mobility of the restricted PIB chains.

3.2 Transport Measurements

Time-evolved infrared (IR) spectra for diffusion experiments were obtained using a Nicolet Research Series Fourier transfer infrared (FTIR) spectrometer with a horizontal attenuated total reflectance (ATR) cell and a zinc selenide trapezoidal ATR crystal or internal reflectance element (IRE). The polymer-coated IRE is mounted in a flow-through ATR cell. The cell consists of two half cells, between which the polymer-coated IRE is placed. The cell is then placed in a horizontal ATR holder and the entire assembly is mounted in the spectrometer. The ATR cell can be temperature regulated by circulating water from a bath through the outside jacket of the cell. The basic Fourier transfer infrared attenuated total reflectance (FT-IR-ATR) Fickian diffusion model developed by Fieldson and Barbari [16–18] was applied to the resultant data.

In this reporting period, we have studied the effect of varying the sulfonation levels in the sulfonated PS-PIB-PS [3] polymer on the transport properties of

12

water and several different alcohols. Alcohols were chosen as penetrants, as they represent small diffusing molecules that vary in both size and polarity.

The time-evolved FT-IR spectra for methanol diffusing through an 8% sulfonated PS-PIB-PS membrane are shown in Figure 12. The characteristic hydroxyl stretch can be seen appearing at 3350 cm^{-1} and increases over time. While other IR bands in this general spectral region may be present due to the strong hydrogen bonding characteristics of the methanol, it is difficult to separate this out in this series of spectra. It should be noted that when the membrane is unsulfonated no diffusion of methanol was detected even after several days.
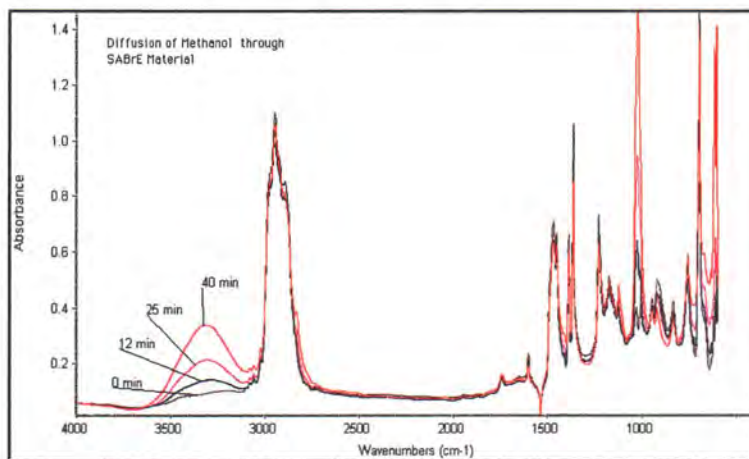

Figure 12. Time-resolved FT-IR spectra for the transport of ethanol through a PS-PIB-PS membrane.

To quantitatively analyze the hydroxyl groups that appear in all four alcohols as well as water, an appropriate baseline was calculated and the peak height was measured. The peak at 3450 cm^{-1} was used as the focus of this study, as this corresponds to the symmetric stretch of the OH functional group. Figure 13 shows the absorbance of the hydroxyl group as a function of time for ethanol through PS-PIB-PS block copolymers at three different sulfonation levels. From a visual inspection, it is clear that the ethanol diffuses much faster through the PS-PIB-PS block copolymer with the highest sulfonation level. The transport through the film appears to vary as a function of the sulfonation level in PS-PIB-PS block copolymers. These data suggest that the sulfonic acid groups enhance the transport rate through the copolymer. The data plotted in Figure 13 are actual calculated IR hydroxyl intensities derived from the time-resolved IR spectra. Therefore, the equilibrium absorbance should be directly related to the amount of ethanol present in the final ethanol/polymer mixture. Examining Figure 13, it is clear that the higher the sulfonation level, the greater the ethanol solubility in the sulfonated PS-PIB-PS.
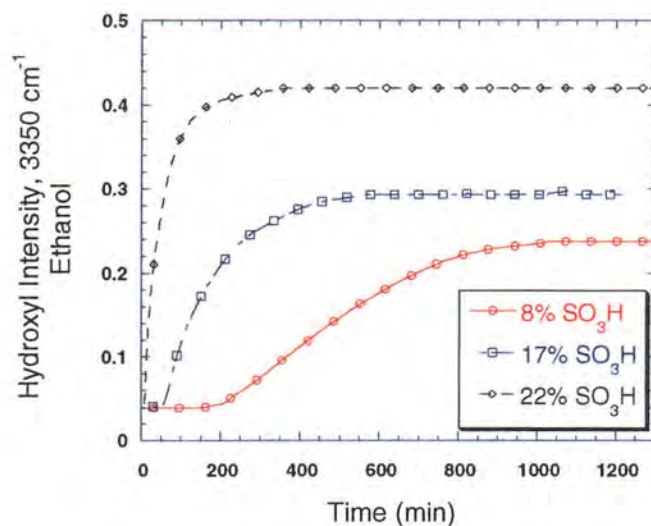
Figure 13. IR intensity vs. time for ethanol through three sulfonated PS-PIB-PS membranes.

Figure 14 shows a comparison of four alcohols diffusing through the sulfonated membrane. The alcohols vary slightly in size. A clear trend is detected that is directly related to the size of the alcohol. The methanol diffuses fastest, while the butanol, the largest alcohol, is shown to diffuse the slowest. The data in Figure 14 are plotted using the absolute IR intensity, where the alcohols with the fastest diffusion rates exhibit the largest band intensities, presumably due to increased solubility of the smaller alcohol molecules.
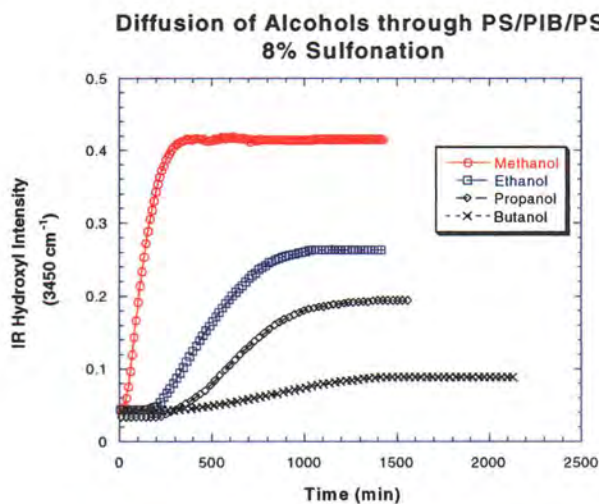

Figure 14. FT-IR absorbance data for the appearance of the 3450 cm^{-1} band of individual alcohols through 8% sulfonated PS-PIB-PS membrane.

14

Figure 15 shows a comparison of four alcohols diffusing through the 22% sulfonated membrane. Similar to Figure 14, molecular transport varies according to the size of the penetrant. Comparing Figure 14 to Figure 15, the absolute intensity of the OH peak is greater for individual alcohols in the spectra of the 22% sulfonated membrane than in the 8% sulfonated membrane. This is a direct result of the increased solubility of the alcohols in the 22% membrane over the 8% membrane.
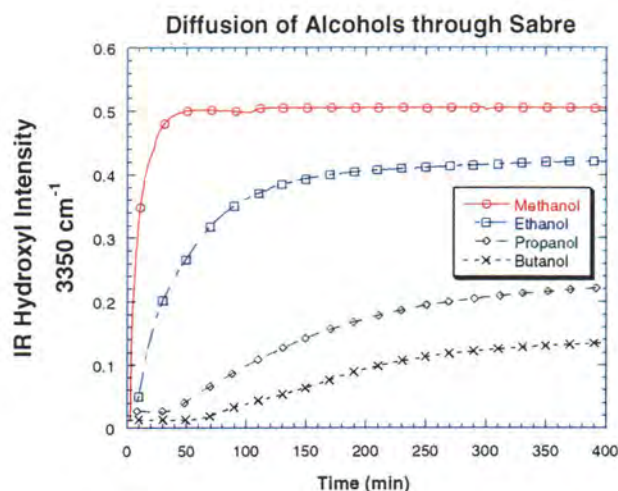

Figure 15. FT-IR absorbance data for the appearance of the 3450 cm^{-1} band for individual alcohols through 22% sulfonated PS-PIB-PS membrane.

Table 1 shows a comparison of the equilibrium sorbtion values for the four alcohols in the sulfonated PS-PIB-PS. Table 1 demonstrates the solubility increase when the sulfonation levels increase. These data confirm the results presented in the FT-IR data that solubility varies as a function of percent sulfonation.

Table 1. Equilibrium sorbtion values for sulfonated PS-PIB-PS membranes.

Solvent	% Uptake by Weight		
	8% S	17% S	22% S
Water	6	9	17
Methanol	36	186	370
Ethanol	34	82	195
n-Propanol	27	34	211
n-Butanol	38	—	—

3.2.1 Diffusion Coefficients

The effective diffusion coefficient was then determined by regressing the integrated absorbance data with an FT-IR-Fickian diffusion model using a least squares regression technique. All of the sulfonated PS-PIB-PS samples displayed Fickian behavior. Figure 16 shows the change in the effective diffusion coefficient with varying sulfonation content for a series of alcohols. The effective diffusion coefficient increases with an increasing sulfonation percentage in the PS-PIB-PS.
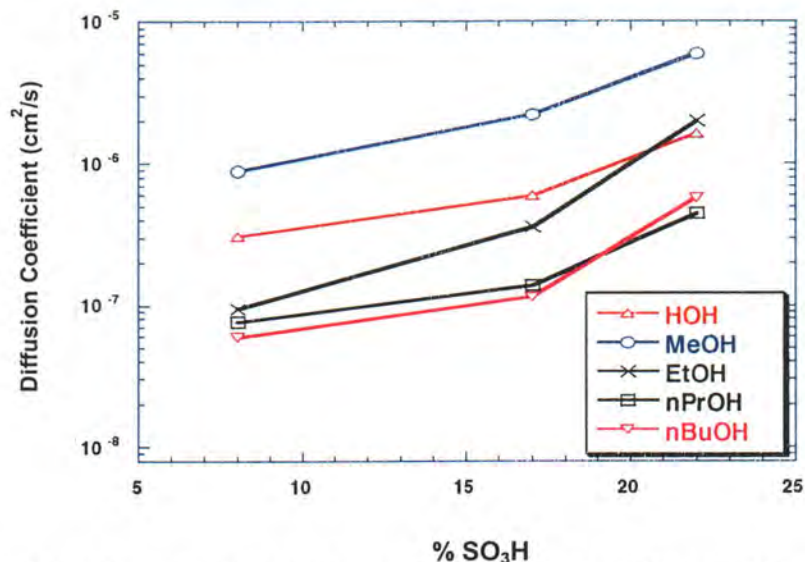

Figure 16. Effect of sulfonation levels on the diffusion coefficients for sulfonated PS-PIB-PS membranes.

One interesting result is in the effective diffusion coefficient of the water. It would seem feasible to suggest that the diffusion coefficient should be faster than methanol because the permeating molecule is so small. However, in all the sulfonated PS-PIB-PS samples, it was found to be slower than methanol yet faster than ethanol. The apparent conflicting trend can be rationalized in terms of the strong hydrogen bonding capability of the water molecules. Water has an unusually high hydrogen bonding solubility component, almost twice that of methanol. This leads to the formation of sorbed water clusters, which decreases the transport rate.

3.2.2 Polymer-Alcohol Interactions

The S = O stretching bands were monitored during the diffusion process to determine if there were any molecular interactions between the water and the polymer. In Figure 17, the time-evolved spectra of the sulfonate functional group, which is part of the sulfonic acid attached to polymer backbone, are shown for the 22% sulfonated PS-PIB-PS sample. IR bands at 1009 cm^{-1} and
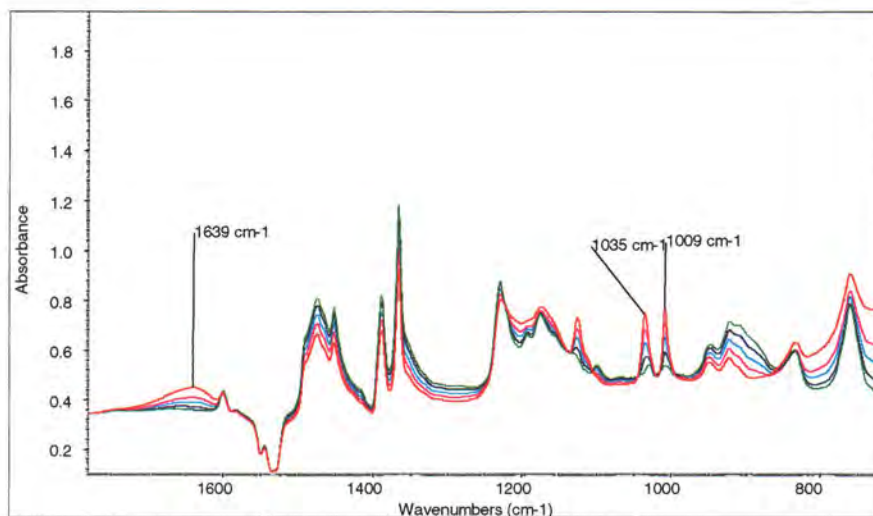
Figure 17. Time-resolved spectra for water diffusing through a 22% sulfonated PS-PIB-PS membrane.

1035 cm^{-1} appear during the diffusion experiment. Neither of these bands can be assigned to any vibrational spectral modes of either polymer or water. These two bands have been reported in the literature [19, 20] to be attributed to a molecular complex formed by an association between the sulfonic acid groups pendant on the polymer backbone and an individual water molecule. The hydrated sulfonic acids are very common structures; they are formed when the acid protonates the H_2O to form a hydronium ion. The associated complex has the form SO_2^- ^+H_3O and has two vibrational component modes, a symmetric stretch and an asymmetric stretch. The 1009 cm^{-1} is assigned to symmetric stretch, and the 1035 cm^{-1} is assigned as an asymmetric stretch.

3.2.3 Ammonium Salt

In an attempt to adjust the transport properties, a chemical exchange of the sulfonic acid proton with an ammonium organic cation was carried out. Figure 18 shows the FT-IR spectral comparison between a 22% sulfonated PS-PIB-PS with that of an ammonium cation exchanged 22% sulfonated PS-PIB-PS. An interesting feature appears in the IR spectrum of the modified polymer—the appearance of two IR bands at 1009 cm^{-1} and 1035 cm^{-1}. These are the same two spectral features that appeared in the self assembling barrier elastomer (SABrE) 22% sulfonation level after diffusing with water. These bands are due to the formation of a molecular complex between the ammonium ion and the sulfonic acid. Clearly, the exact nature of the complex formed when sulfonic acids interact with various cations does not change the position of the IR bands. It does however give a clear indication of formation of such complexes.
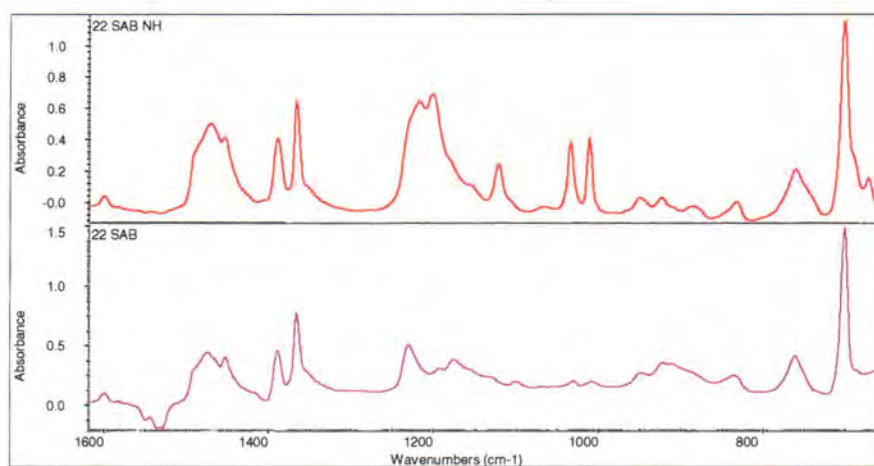
17

Figure 18. Comparison of the FT-IR spectra of a 22% sulfonated PS-PIB-PS (bottom spectrum) with that of an ammonium cation exchanged 22% sulfonated PS-PIB-PS (top spectrum).

In an attempt to identify which solvent molecules used in this study formed molecular complexes with the 22% sulfonated PS-PIB-PS, FT-IR spectra for each solvent-swollen complex was assessed to determine the presence of 1009 cm^{-1} and 1035 cm^{-1} bands. In each case, these features were identified, as shown in Figure 19, which leads to the conclusion that small molecular weight alcohols form complexes with the 22% sulfonated PS-PIB-PS polymer.
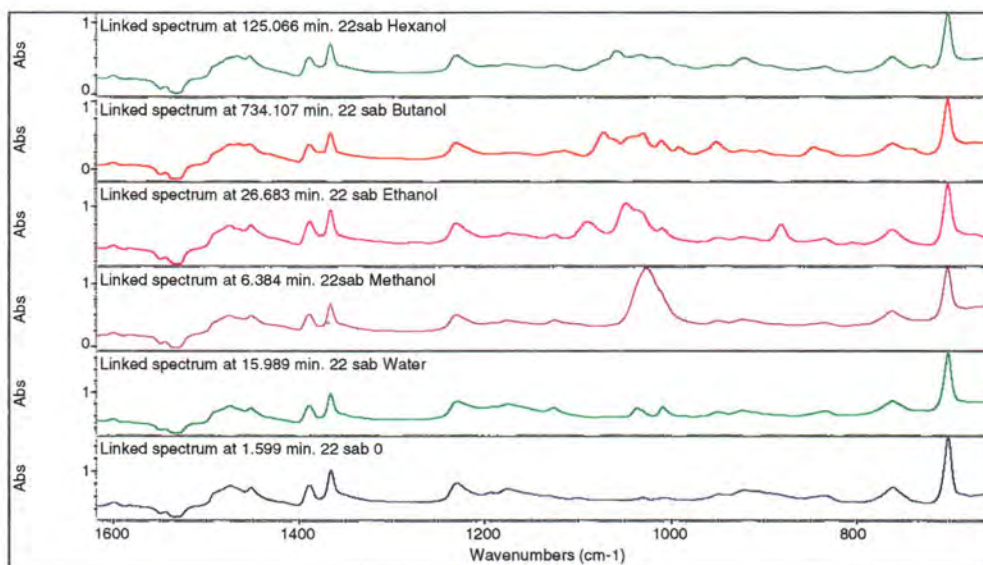

Figure 19. Comparison of the FT-IR spectra of a 22% sulfonated PS-PIB-PS swollen with various solvents.

3.2.4 Transport Properties of the Ammonium Exchanged Polymer

Figure 20 shows the diffusion rate curves for the transport of five individual alcohols through the ammonium exchanged SABrE material. The rate curves follow the same trends exhibited by the 22% sulfonated PS-PIB-PS, where the solvent size dictates the rate of transport through the polymer membrane.
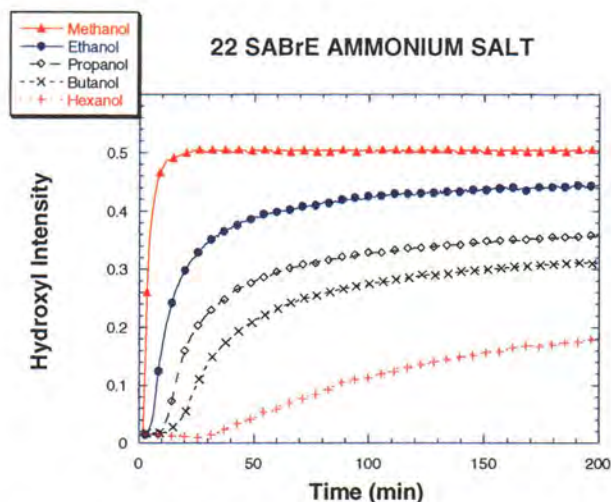

Figure 20. Comparison of the FT-IR spectra of a 22% sulfonated PS-PIB-PS swollen with various solvents.

The effective diffusion coefficient calculated for the ammonium exchanged SABrE materials are slightly higher than those calculated for the 22% sulfonated PS-PIB-PS polymer. Figure 21 shows the relationship of the exchanged material to that of the base SABrE polymers. The exchanged SABrE material demonstrated faster transport properties for each corresponding alcohol than the other base polymers.
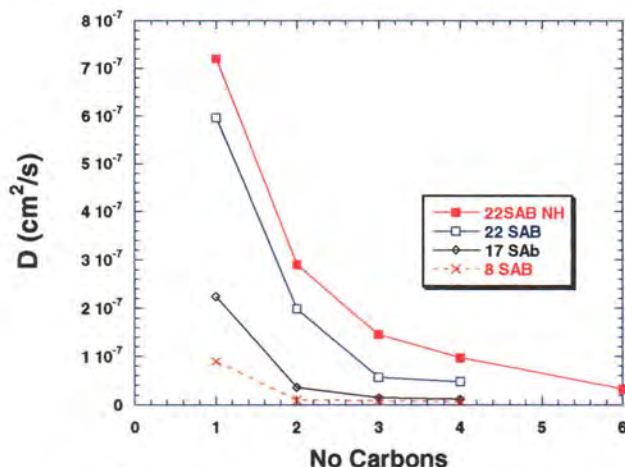

Figure 21. Comparison of the diffusion coefficient with the size of diffusing alcohol molecule.

One reason for this might be that the formation of the solvent-sulfonic acid complex. In the ammonium exchanged SABrE material, this complex already exists, while in the case of the 22% sulfonated PS-PIB-PS base material, the complex is formed followed by diffusion of the uncomplexed water molecules.

Figure 22 shows the diffusion rate curve for the transport of water through the 22% sulfonated PS-PIB-PS base material. The figure shows that the hydronium complex forms first. The unassociated water molecules diffuse through the membrane soon after the complex forms.
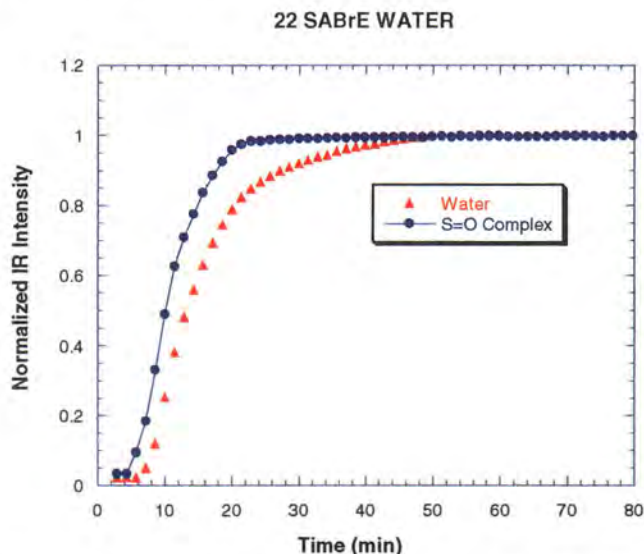

Figure 22. The diffusion rate curve for the transport of water through the 22% sulfonated PS-PIB-PS base material.

3.3 Solubility

The unmodified triblock copolymer and the sulfonated forms of the polymer were evaluated for solubility in a range of solvents. This was a qualitative study in which 50–100 mg of polymer was placed into 10–15 ml of solvent for 24 hr. If the sample did not dissolve, the polymer was left for an additional 24 hr, at which time the solvent effect was recorded based on visual inspection. The results of the solubility experiments are shown in Table 2.

3.4 Processing

The relative ease at which the triblock copolymers dissolve in common solvents allowed a variety of processing investigations to be performed. Polymer solutions were prepared at 5% concentration. The solvent or combination of solvents used depended on the level of sulfonation in the copolymer. TS3000S and the copolymers sulfonated to 5% and 8% were prepared by dissolving the

Table 2. Solubility of triblock copolymers.

Solvent	TS3000S	PS	PIB	Sulfonated TS3000S (SABrE)				
				8%	17%	22%	26%	22%-AM
Water	N	N	N	N	N	N	N	N
Acetonitrile	N	N	N	N	N	N	N	N
Cyclohexane	Y	X	Y	Y	X	N	Y	N
Acetone	N	X	N	N	N	N	N	N
Methanol	N	N	N	N	N	N	N	N
Tetrahydrofuran	Y	Y	Y	Y	Y	Y	Y	Y
Methyl ethyl ketone	X	Y	N	X	X	X	X	N
Methylene chloride	Y	Y	X	Y	Y	X	Y	Y
Ethanol	N	N	N	N	N	N	N	N
N, N dimethylformamide	N	Y	N	N	N	N	N	N
n-Propanol	N	N	N	N	N	N	N	N
1, 5 dichloropentane	Y	Y	N	X	N	N	N	N
n-Decane	Y	N	Y	N	N	N	N	N
Hexane	Y	N	Y	N	N	N	N	N
Carbon tetrachloride	Y	Y	Y	Y	Y	X	Y	X
Benzene	Y	Y	Y	Y	Y	Y	Y	X
Cyclohexanol	Y	X	Y	Y	N	N	X	N
n-Butanol	N	N	N	N	N	X	X	N
Ethylene glycol	N	N	N	N	N	N	N	N
Dimethylsulfoxide	N	N	N	N	N	N	N	N
Toluene	Y	Y	Y	Y	Y	Y	Y	X
1-Methyl-2-Pyrrolidinone	N	Y	N	N	N	N	N	N
Acrylonitrile	N	X	N	N	N	N	N	N
Triethyl phosphonate	N	Y	N	N	N	N	N	N
Dimethyl methyl phosponate	N	N	N	N	N	N	N	N

Y= sample mostly dissolves.
N= sample does not dissolve.
X = sample partially dissolves/decomposes.

copolymers in 100% toluene. Solutions prepared with copolymers comprised of greater percentages of sulfonation were prepared using mixed solvents of 85% toluene and 15% hexyl alcohol. The hexyl alcohol was required to solvate the sulfonated PS domains. Films were then prepared by casting 25 ml of the polymer solution into 4-in-diameter teflon petri dishes and allowed to dry under a hood. The films were then placed in a vacuum oven at 50 °C and continued to dry for approximately two weeks to remove trace solvents. The resulting films were transparent, with a relatively homogeneous thickness of approximately 4 mil.

Coated fabrics were prepared using several methods. Woven fabrics were provided by Mr. Quoc Truong and included a gray 5 oz/yd^2 NYCO 50/50 cotton/nylon woven fabric without Quarpel treatment and the MIL-C-44436 [21] 6.7 oz/yd^2 JSLIST shell fabric (with Quarpel treatment). In the first coating method, 4-in-diameter samples of woven fabric were cut and placed in the bottom of the petri dishes. Approximately 25 ml of 5% polymer solution was poured over the fabric, and the films were allowed to dry according to this procedure. This resulted in a smooth, uniform, and relatively thick (~4 mil) coating of the fabric, with the coating forming primarily on one side of the woven fabric. Adherence of the coating to the surface of the woven fabric appears to be good.

The second method of coating the woven fabric involved a "dip coating" method. In this case, the polymer solutions were poured into a shallow dish, and the woven fabrics were dipped into the coating and held there for approximately 20 s and then hung to dry under the hood. This method produced a very thin coating on the fabric, and in the case of the gray 50/50 cotton/nylon fabric, a homogeneous film did not form; however, the fibers of the fabric were coated. When this fabric was dipped, the solution immediately permeated the thickness of the fabric, and it appeared that the polymer coating would be formed on both sides of the fabric. This was in part due to the relatively loose weave of the fabric. The thickness and weave of the MIL-C-44436 [21] fabric allowed the dipped fabric to be coated on the dipped side only. That is, the polymer solution did not appear to permeate to the other side of the fabric when the fabric was laid on top of the polymer solution. This fabric was coated on the back (noncamouflaged) side of the fabric. This seems to be the preferred method of coating the camouflaged fabric, since the polymer coating in this case will not change the appearance or gloss of the camouflage pattern. The copolymer did appear to form a more continuous film on the MIL-C-44436 [21] fabric compared to the coated 50/50 cotton/nylon fabric. Additional fabrics were dip coated a second and third time, with a 15-min dry time in between coats, in an effort to increase the film thickness and improve the quality of the film. Both the 50/50 cotton/nylon fabric and the MIL-C-44436 [21] fabric appear to have continuous films formed on the surface after three subsequent dips in the polymer solution. Because these films were very thin, accurate measurements of film thickness could not be obtained for films formed after one or two dips. However, films formed after three dips in the polymer solution are estimated to be a maximum of 2 mil thick.

Finally, 5% polymer solutions were spray coated onto one side of both woven fabrics. A conventional air gun was utilized. After spraying, the coated fabrics were allowed to dry under a hood. A homogeneous film appeared to be formed on the MIL-C-44436 [21] fabric; however, the coating appears to be very thin. Future work on spray coating the fabrics will involve increasing the

concentration of the polymer solution in an effort to increase the film thickness. The first coating method described, casting the film onto the fabric in a petri dish, produced the thickest and smoothest coating. Samples of the different films and coated fabrics are provided to SBCCOM-Natick for further evaluation.

The processing investigations demonstrated that elastomeric membrane films and coated fabrics can be produced using common solvents and simple solution processing procedures, indicating that scale-up of these processing techniques should be economically feasible. Further work will address optimization of the coated films to achieve homogeneous, defect-free coatings and will involve developing test methodology to determine that the coated fabrics are continuous and free of pores. Collaborative work with SBCCOM-Natick should be conducted to determine the performance of the coated fabrics and to provide insight into the required parameters for coating optimization.

4. Conclusions

In this reporting period, the morphology, viscoelastic, and transport properties of the PS-PIB-PS triblock copolymer were investigated with respect to sulfonation level and counter-ion substitution. DMA showed that sulfonation levels of 5% and 8% did not affect the dynamic storage modulus E'. However, sulfonation levels of 12%, 14%, 17%, and 22% resulted in a significant increase in E' above the glass transition. SAXS results confirmed that between 8% and 12% sulfonation, a phase transition occurs from hexagonally packed cylinders to lamellar structure, respectively. This phase transition is the result of swelling of the styrene domains caused by the higher sulfonation levels. SAXS data indicates that the lamellar structure is aligned parallel to the film plane, which is consistent with the increase in dynamic storage modulus that is measured with the film in tension. Increasing the sulfonation level allows greater interaction between sulfonic acid groups via hydrogen bonding, creating noncovalent crosslinks in the styrene domains and thereby increasing the rubbery plateau modulus. The impact of the higher sulfonation levels on polymer morphology primarily affects the viscoelastic properties of the rigid styrenic domains. The major component of the PS-PIB-PS triblock copolymer is comprised of flexible PIB. The dynamic loss modulus E" showed that increasing the sulfonation level does not adversley affect the viscoelastic response of the PIB mid-block. The triblock copolymer retains its low temperature flexibility and elastomeric behavior, regardless of sulfonation level, exhibiting a Tg of approximately $-63\,^{\circ}C$.

Transport measurements confirm that the sulfonation level directly dictates the transport rate of small molecules (alcohol and water) through the PS-PIB-PS triblock copolymer membrane. Faster water transport can be achieved by incorporating more sulfonic acid groups throughout the polymer backbone. Additionally, the IR spectral intensity of the hydroxyl band can be related to the total solubility of alcohol in the polymer. This effect is confirmed by swelling experiments. Finally, the IR data clearly identifies molecular interactions between the solvating alcohol molecules and the PS-PIB-PS triblock copolymer. The observed properties of these polymers, coupled with their ease of processing, suggest that the ion containing block copolymers are worthy of further development as potential candidates for chemical protective clothing.

5. References

1. Lee, B. L., T. W. Yang, and E. Wilusz. "Moisture Effects on Isobutylene-Isoprene Copolymer-Based Composite Barrier. 1. Moisture Diffusion and Detection." *Polymer Engineering & Science*, vol. 36, no. 9, p. 1217, 1996.

2. Lu, X. Y., W. P. Steckle, Jr., and R. A. Weiss. "Morphological Studies of a Triblock Copolymer Ionomer by Small-Angle X-Ray Scattering." *Macromolecules*, vol. 26, no. 24, p. 6525, 1993.

3. Reuschle, D. A., D. A. Mountz, L. B. Brister, R. F. Storey, and K. A. Mauritz. "Thermal Analysis of Poly(styrene-co-isobutylene-co-styrene) Block Copolymers and Block Copolymer Ionomers." *ACS Polymer Preprints*, vol. 39, p. 383, 1997.

4. Weiss, R. A., A. Sen, L. A. Pottick, and C. L. Willis. "Block Copolymer Ionomers—Thermoplastic Elastomers Possessing Two Distinct Physical Networks." *Polymer Communication*, vol. 31, no. 6, p. 220, 1990.

5. Mani, S., R. A. Weiss, C. E. Williams, and S. F. Hahn. "Microstructure of Ionomers Based on Sulfonated Block Copolymers of Polystyrene and Poly(Ethylene-Alt-Propylene)." *Macromolecules*, vol. 32, no. 11, p. 3663, 1999.

6. Crawford, D., E. Napadensky, N. Beck Tan, J. Sloan, D. Reuschle, D. Mountz, K. Mauritz, K. Laverdure, S. Gido, W. Liu, and B. Hsiao. "Semi-Permeable Membrane From Ionomeric Self-Assembled Block Copolymer." ARL-TR-2403, U.S. Army Research Laboratory, Aberdeen Proving Ground, MD, February 2001.

7. Hamley, I. W. *The Physics of Block Copolymers*. New York, NY: Oxford University Press, 1998.

8. Lu, X. Y., W. P. Steckle, and R. A. Weiss. "Ionic Aggregation in a Block-Copolymer Ionomer." *Macromolecules*, vol. 26, no. 22, pp. 5876–5884, 1993.

9. David, J. L., S. P. Gido, K. L. Hong, J. Mays, and N. Beck Tan. "Core-Shell Cylinder Morphology in Poly(styrene-b-1,3-cyclohexadiene) Diblock Copolymers." *Macromolecules*, vol. 32, no. 10, pp. 3216–3226, 1999.

10. Beamish, A., R. A. Goldberg, and D. J. Hourston. "Effect of Casting Solvents on Certain Physical Properties of ABA Poly(styrene-b-butadiene) Copolymers." *Polymer*, vol. 18, no. 1, pp. 49–54, 1977.

11. Pedemonte, E., and G. C. Alfonso. "Morphology of Polystyrene-Polybutadiene-Polystyrene 3-Block Copolymers." *Macromolecules*, vol. 8, no. 1, p. 85, 1975.

12. Baugh, D. W. "Morphological & Physical Characterization of Poly(styrene-isobutylene-styrene) Block Copolymers and Ionomers Thereof." Ph.D. thesis, University of So. Mississippi, Hattiesburg, MS, August 1997.

13. Eisenberg, A., B. Hird, and R. B. Moore. "A New Multiplet-Cluster Model for the Morphology of Random Ionomers." *Macromolecules*, vol. 23, no. 18, p. 4098, 1990.

14. Hara, M., P. Jar, and J. A. Sauer. "Dynamic Mechanical-Properties of Sulfonated Polystyrene Ionomers." *Polymer*, vol. 32, no. 9, p. 1623, 1991.

15. Calhoun, B. H., and R. B. Moore. "Crystallization Kinetics Of Lightly Sulfonated Syndiotactic Polystyrene Ionomers." *Journal of Vinyl & Addition Technology*, vol. 2, p. 358, 1996.

16. Elabd, Y. A., J. M. Sloan, and T. A. Barbari. "Diffusion of Acetonitrile in Conformational Isomers of an H12MDI Polyurethane." *Polymer*, vol. 41, no. 6, p. 2203, March 2000.

17. Fieldson, G. T., and T. A. Barbari. "The Use of FTIR-ATR Spectroscopy to Characterize Penetrant Diffusion in Polymers." *Polymer*, vol. 34, no. 6, p. 1146, 1993.

18. Fieldson, G. T., and T. A. Barbari. "Analysis of Diffusion in Polymers Using Evanescent Field Spectroscopy." *AIChE Journal*, vol. 41, no. 4, p. 795, 1995.

19. Colthrup, N, L. H. Daily, and S. E. Wiberly. *Introduction to Infrared and Raman Spectroscopy*. 3rd ed., New York, NY: Academic Press, 1990.

20. Detoni, S., and D. Hadzi. "Infra-Red Spectra of Some Organic Sulphur-Oxygen Compounds." *Spectrochimica Acta*, vol. 11, p. 601, 1957.

21. U.S. Army Natick Research, Development, and Engineering Center. "Cloth, Camouflage Pattern, Wind Resistant Poplin, Nylon/Cotton Blend." Natick, MA, 13 July 1992.

NO. OF COPIES	ORGANIZATION
2	DEFENSE TECHNICAL INFORMATION CENTER DTIC OCA 8725 JOHN J KINGMAN RD STE 0944 FT BELVOIR VA 22060-6218
1	HQDA DAMO FDT 400 ARMY PENTAGON WASHINGTON DC 20310-0460
1	OSD OUSD(A&T)/ODDR&E(R) DR R J TREW 3800 DEFENSE PENTAGON WASHINGTON DC 20301-3800
1	COMMANDING GENERAL US ARMY MATERIEL CMD AMCRDA TF 5001 EISENHOWER AVE ALEXANDRIA VA 22333-0001
1	INST FOR ADVNCD TCHNLGY THE UNIV OF TEXAS AT AUSTIN 3925 W BRAKER LN STE 400 AUSTIN TX 78759-5316
1	DARPA SPECIAL PROJECTS OFFICE J CARLINI 3701 N FAIRFAX DR ARLINGTON VA 22203-1714
1	US MILITARY ACADEMY MATH SCI CTR EXCELLENCE MADN MATH MAJ HUBER THAYER HALL WEST POINT NY 10996-1786
1	DIRECTOR US ARMY RESEARCH LAB AMSRL D DR D SMITH 2800 POWDER MILL RD ADELPHI MD 20783-1197

NO. OF COPIES	ORGANIZATION
1	DIRECTOR US ARMY RESEARCH LAB AMSRL CI AI R 2800 POWDER MILL RD ADELPHI MD 20783-1197
3	DIRECTOR US ARMY RESEARCH LAB AMSRL CI LL 2800 POWDER MILL RD ADELPHI MD 20783-1197
3	DIRECTOR US ARMY RESEARCH LAB AMSRL CI IS T 2800 POWDER MILL RD ADELPHI MD 20783-1197

ABERDEEN PROVING GROUND

| 2 | DIR USARL AMSRL CI LP (BLDG 305) |

8   USA NATICK SOLDIER SYS CTR
        SBCCOM DR
        N SCHNEIDER
        Q TRUONG
        D RIVIN
        J WALKER
        E WILUSZ
        W ZUKAS
        M SENNETT
        J VARNUM
        KANSAS ST
        NATICK MA 01760

ABERDEEN PROVING GROUND

30   DIR USARL
        AMSRL WM MA
          E NAPADENSKY (30 CPS)

REPORT DOCUMENTATION PAGE

Form Approved
OMB No. 0704-0188

1. AGENCY USE ONLY (Leave blank)	2. REPORT DATE	3. REPORT TYPE AND DATES COVERED
	May 2001	Final, October 1999–October 2000

4. TITLE AND SUBTITLE	5. FUNDING NUMBERS
Viscoelastic and Transport Properties of Sulfonated PS-PIB-PS Block Copolymers	622105.AH84

6. AUTHOR(S)

Eugene Napadensky, Dawn Crawford, James Sloan, and Nora Beck Tan

7. PERFORMING ORGANIZATION NAME(S) AND ADDRESS(ES)	8. PERFORMING ORGANIZATION REPORT NUMBER
U.S. Army Research Laboratory ATTN: AMSRL-WM-MA Aberdeen Proving Ground, MD 21005-5069	ARL-TR-2482

9. SPONSORING/MONITORING AGENCY NAMES(S) AND ADDRESS(ES)	10. SPONSORING/MONITORING AGENCY REPORT NUMBER

11. SUPPLEMENTARY NOTES

12a. DISTRIBUTION/AVAILABILITY STATEMENT	12b. DISTRIBUTION CODE
Approved for public release; distribution is unlimited.	

13. ABSTRACT (Maximum 200 words)

Morphology, viscoelastic, and transport properties of the sulfonated polystyrene-polyisobutylene-polystyrene (PS-PIB-PS) block copolymer were investigated with respect to sulfonation level and counter-ion substitution. Dynamic mechanical analysis (DMA) was used to examine the dynamic storage modulus E' and dynamic loss modulus E", as they relate to changes in sulfonation levels. Small-angle x-ray scattering (SAXS) results confirmed that at a certain percent of sulfonation, a phase transition occurs from hexagonally packed cylinders to lamellar structure due to swelling of the styrene domains caused by the higher sulfonation levels. Transport measurements using Fourier Transfer Infrared Spectrometer (FTIR) confirm that the sulfonation level directly dictates the transport rate of small molecules (alcohol and water) through the PS-PIB-PS triblock copolymer membrane. Faster water transport can be achieved by incorporating more sulfonic acid groups throughout the polymer backbone. In addition, infrared (IR) data clearly identifies molecular interactions between the solvating alcohol molecules and the PS-PIB-PS triblock copolymer. The observed properties suggest that these ion-containing block copolymers are worthy of further development as barrier membranes to be incorporated into chemical protective clothing.

14. SUBJECT TERMS		15. NUMBER OF PAGES
transport, DMA, morphology, triblock, copolymer, sulfonated polystyrene, x-ray scattering, FT-IR, diffusion, ionomers, polystyrene-polyisobutylene, membrane		35
		16. PRICE CODE

17. SECURITY CLASSIFICATION OF REPORT	18. SECURITY CLASSIFICATION OF THIS PAGE	19. SECURITY CLASSIFICATION OF ABSTRACT	20. LIMITATION OF ABSTRACT
UNCLASSIFIED	UNCLASSIFIED	UNCLASSIFIED	UL

USER EVALUATION SHEET/CHANGE OF ADDRESS

This Laboratory undertakes a continuing effort to improve the quality of the reports it publishes. Your comments/answers to the items/questions below will aid us in our efforts.

1. ARL Report Number/Author __ARL-TR-2482 (Napadensky)__ Date of Report __May 2001__

2. Date Report Received_____

3. Does this report satisfy a need? (Comment on purpose, related project, or other area of interest for which the report will be used.) _____

_____

4. Specifically, how is the report being used? (Information source, design data, procedure, source of ideas, etc.)_____

_____

_____

5. Has the information in this report led to any quantitative savings as far as man-hours or dollars saved, operating costs avoided, or efficiencies achieved, etc? If so, please elaborate._____

_____

_____

6. General Comments. What do you think should be changed to improve future reports? (Indicate changes to organization, technical content, format, etc.)_____

_____

_____

_____

CURRENT
ADDRESS

Organization _____

Name _____ E-mail Name _____

Street or P.O. Box No. _____

City, State, Zip Code _____

7. If indicating a Change of Address or Address Correction, please provide the Current or Correct address above and the Old or Incorrect address below.

OLD
ADDRESS

Organization _____

Name _____

Street or P.O. Box No. _____

City, State, Zip Code _____

(Remove this sheet, fold as indicated, tape closed, and mail.)
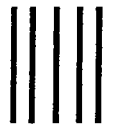**(DO NOT STAPLE)**

DEPARTMENT OF THE ARMY

OFFICIAL BUSINESS

BUSINESS REPLY MAIL
FIRST CLASS PERMIT NO 0001, APG, MD

POSTAGE WILL BE PAID BY ADDRESSEE

DIRECTOR
US ARMY RESEARCH LABORATORY
ATTN AMSRL WM MA
ABERDEEN PROVING GROUND MD 21005-5069